Electronic Supplementary Material (ESI) for Journal of Materials Chemistry A.


# Kinetics-Mediated Assembly Assisted Precise Synthesis of Magnetic Ordered Mesoporous Carbon Nanospheres for Ultra-Efficient Electromagnetic Wave Absorption

Mengmeng Wei,[a, b] Kai Liu,[c] Qingyan Li,[a] Hongwei Zhang,[a] Guoxian Zhang,[a] Qiuyu Zhang [*a, b] and Baoliang Zhang [*a, d]

[a] School of Chemistry and Chemical Engineering, Northwestern Polytechnical University, Xi'an, 710072, China.

[b] Xi'an Key Laboratory of Functional Organic Porous Materials, Northwestern Polytechnical University, Xi'an, 710129, China.

[c] School of Materials Science and Engineering, Peking University, Beijing 100871, China.

[d] Shaanxi Engineering and Research Center for Functional Polymers on Adsorption and Separation, Sunresins New Materials Co. Ltd., Xi'an, 710072, China.

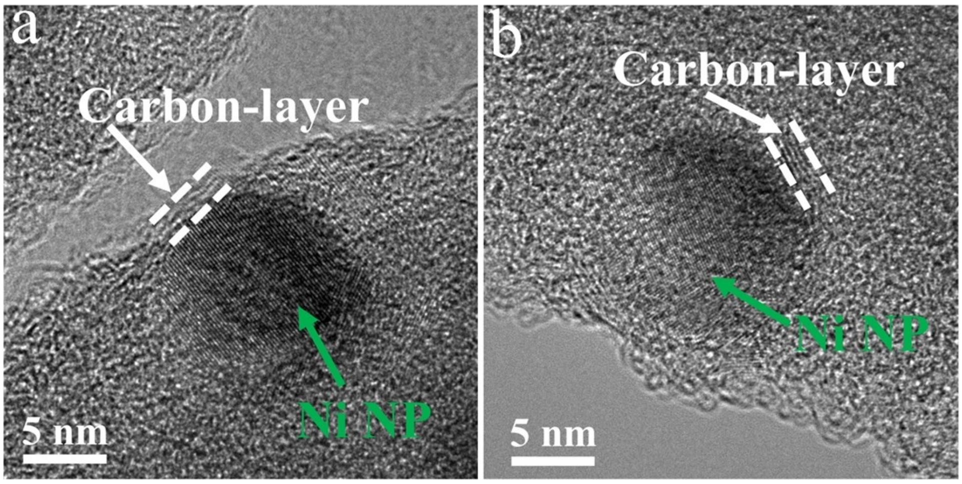


**Figure S1.** High-resolution TEM images Ni/OMCN-D (a) and Ni/OMCN-S (b).

[*] Corresponding author, Northwestern Polytechnical University, Youyi Road 127#, Xi'an (710072), China. Email: qyzhang@nwpu.edu.cn; blzhang@nwpu.edu.cn

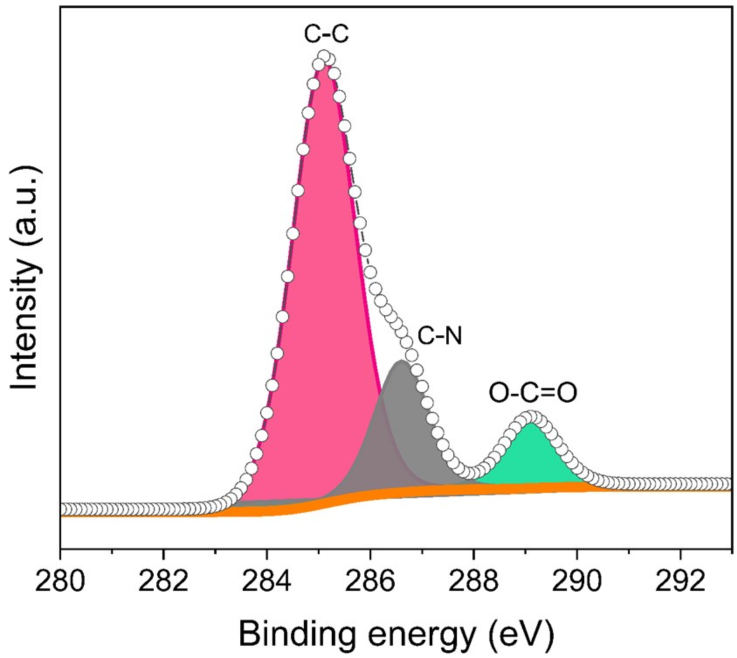


**Figure S2.** C 1s spectrum of Ni/OMCN-D.

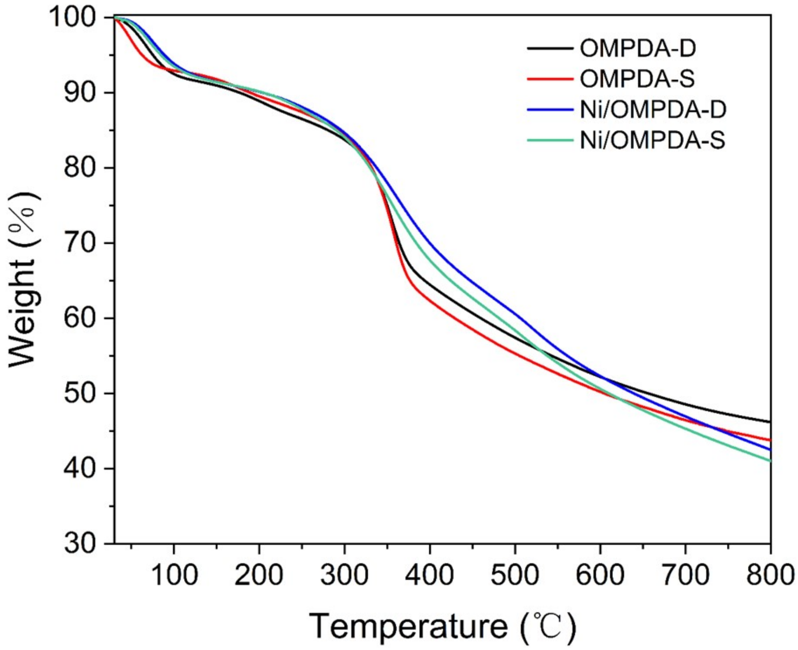


**Figure S3.**TGA curves of the samples under nitrogen atmosphere.

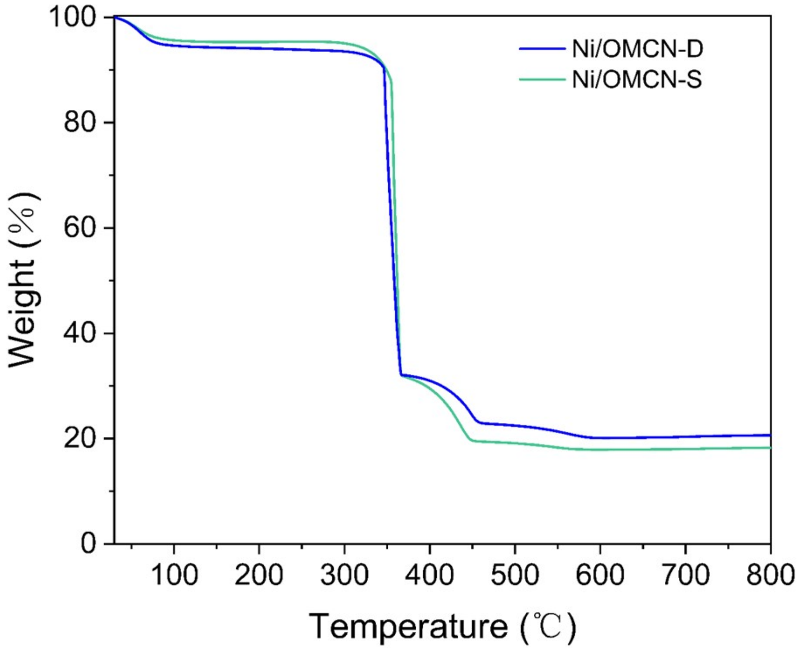


**Figure S4.**TGA curves of Ni/OMCN-D and Ni/OMCN-S under air atmosphere.

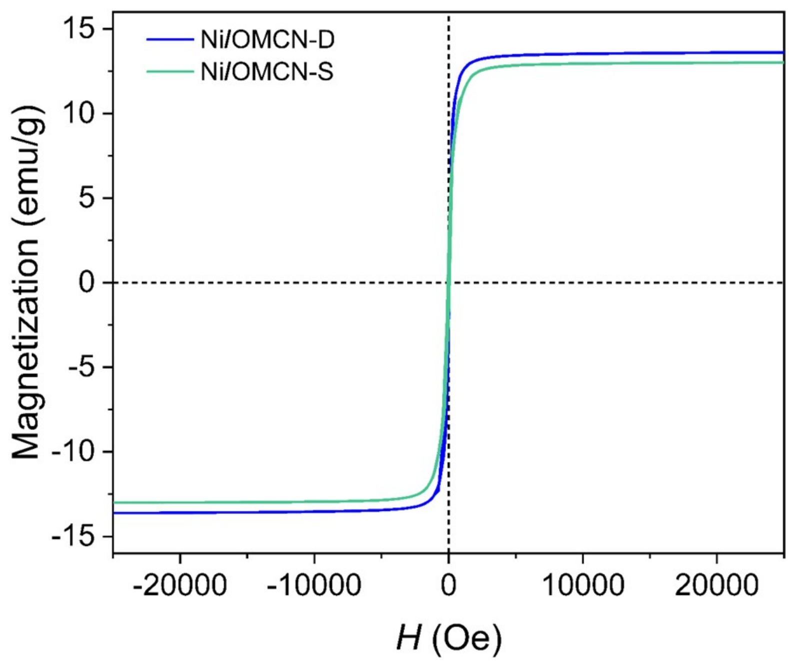


**Figure S5.** Room-temperature hysteresis loops of Ni/OMCN-D and Ni/OMCN-S.

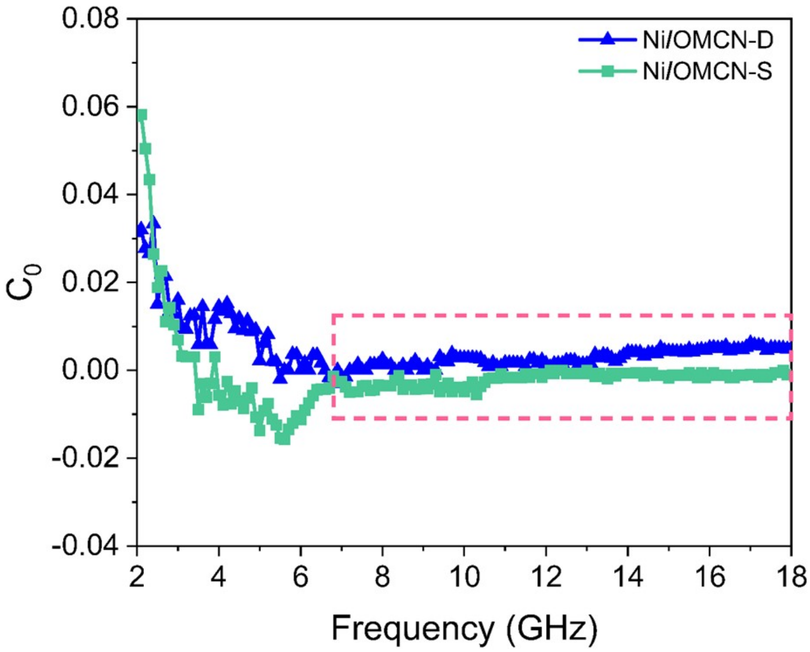


**Figure S6.** $C_0$-*f* curves of Ni/OMCN-D and Ni/OMCN-S.

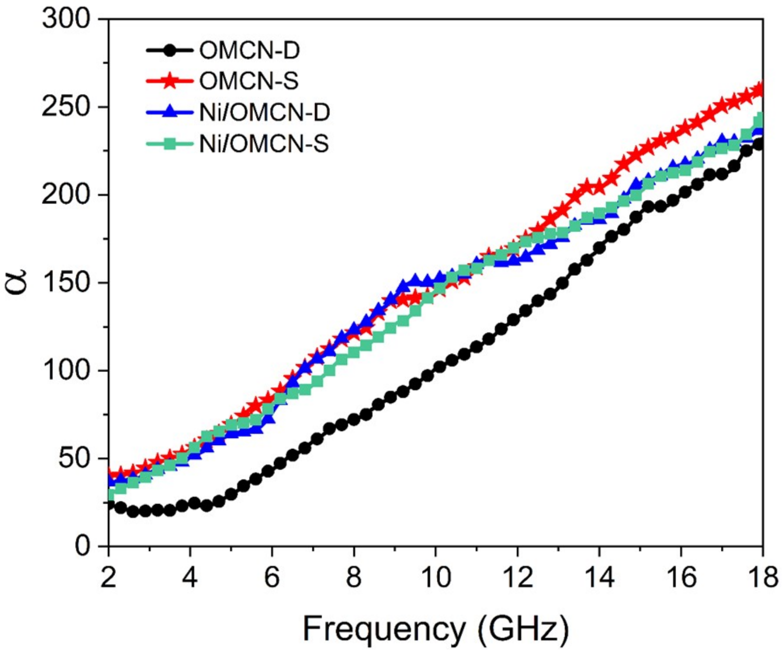


**Figure S7.** Attenuation constant of the samples.

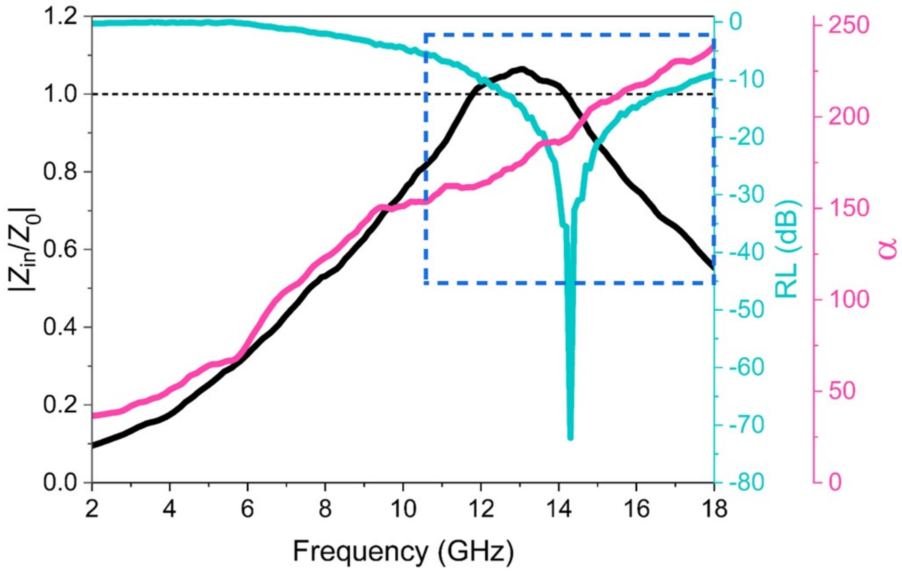


**Figure S8.** The frequency-dependent RL, $|Z_{in}/Z_0|$ and α values of the Ni/OMCN-D composite at the 2.0 mm thickness.

Ni/OMCN-D was taken as an example to reveal the intrinsic relationships between impedance matching, dissipation capability and EMWA performance. The EMWA properties of Ni/OMCN-D at 2.0 mm were analyzed by examining the variation in RL, $|Z_{in}/Z_0|$ and α as a function of frequency (Figure S8). When the frequency was 18 GHz, α reach the maximum value of 239, while the corresponding RL intensity decreased to the lowest level due to poor impedance matching revealed by $|Z_{in}/Z_0|$. The $|Z_{in}/Z_0|$ value of Ni/OMCN-D was nearest to 1 at 12.0 and 14.3 GHz. Interestingly, Ni/OMCN-D showed an extremely high RL value of -72.2 dB at 14.3 GHz, whereas RL intensify at 12.0 GHz was comparatively low because of the inferior dissipation ability verified by the lower α. From the above result, it was good impedance matching and sufficient dissipation capability that synergistically determine excellent EMWA properties.

**Table S1.** Physicochemical properties of the samples.

| Sample | $S_{BET}$ ($m^2$ $g^{-1}$) | $V_{total}$ ($cm^3$ $g^{-1}$) | $D_{pore}$ (nm) | $I_D/I_G$ | N content (wt%) |
|---|---|---|---|---|---|
| OMCN-D | 313 | 0.21 | 8.9 | 0.98 | 3.2 |
| OMCN-S | 309 | 0.32 | 9.6 | 0.98 | 2.9 |
| Ni/OMCN-D | 395 | 0.43 | 9.7 | 1.0 | 2.5 |
| Ni/OMCN-S | 400 | 0.46 | 10.3 | 1.0 | 2.3 |

**Table S2.** EMWA performance of the relative absorbers.[1-12]

| Sample | Filler loading (wt %) | $RL_{max}$ (dB) | Thickness (mm) | EAB (GHz) | Ref. |
|---|---|---|---|---|---|
| NC@NCNTs | 30 | -41.5 | 1.5 | 5.2 | 1 |
| HBN-Co/C | - | -42.3 | 1.7 | 5.1 | 2 |
| HPCMCs | 30 | -60.7 | 3.2 | 3.9 | 3 |
| NHCS@NiO/Ni | 12 | -44.0 | 1.7 | 4.38 | 4 |
| Ni-SA/HPCF | 10 | -53.2 | 3.5 | 5.0 | 5 |
| NiFe@C@GO | 30 | -51.0 | 2.8 | 3.97 | 6 |
| GMFs | 10 | -42.9 | 4.0 | 5.59 | 7 |
| Co/C | 40 | -35.3 | 2.5 | 5.8 | 8 |
| BLCNs | 20 | -45.3 | 1.5 | 4.2 | 9 |
| NC | 9 | -24.0 | 1.6 | 6.0 | 10 |
| MCHS | 20 | -50.9 | 3.2 | 5.4 | 11 |
| $Fe_3C$@C | 20 | -57.6 | 3.95 | 5.0 | 12 |
| Ni/OMCN-D | 25 | -72.2 | 2.0 | 5.6 | Herein |
| Ni/OMCN-S | 25 | -47.1 | 1.9 | 6.2 | Herein |

## References


1 D. Liu, Y. Du, P. Xu, F. Wang, Y. Wang, L. Cui, H. Zhao and X. Han, *J. Mater. Chem. A*, 2021, **9**, 5086-5096.

2 J. Liang, J. Chen, H. Shen, K. Hu, B. Zhao and J. Kong, *Chem. Mat.*, 2021, **33**, 1789-1798.

3 H. Zhao, X. Xu, Y. Wang, D. Fan, D. Liu, K. Lin, P. Xu, X. Han and Y. Du, *Small*, 2020, **16**, 2003407.

4 B. Li, Z. Ma, X. Zhang, J. Xu, Y. Chen, X. Zhang and C. Zhu, *Small*, 2023, **19**, 2207197.

5 X. Zhang, B. Li, J. Xu, X. Zhang, Y. Shi, C. Zhu, X. Zhang and Y. Chen, *Adv. Funct. Mater.*, 2023, **33**, 2210456.

6 Z. Yang, H. Lv and R. Wu, *Nano Res.*, 2016, **9**, 3671-3682.

7 C. Chen, J. Xi, E. Zhou, L. Peng, Z. Chen and C. Gao, *Nano-Micro Lett.*, 2017, **10**, 26.

8 Y. Lü, Y. Wang, H. Li, Y. Lin, Z. Jiang, Z. Xie, Q. Kuang and L. Zheng, *Acs Appl. Mater. Interfaces*, 2015, **7**, 13604-13611.

9 J. Fu, W. Yang, L. Hou, Z. Chen, T. Qiu, H. Yang and Y. Li, *Ind. Eng. Chem. Res.*, 2017, **56**, 11460-11466.

10 H. Zhao, Y. Cheng, H. Lv, B. Zhang, G. Ji and Y. Du, *Acs Sustain. Chem. Eng.*, 2018, **6**, 15850-15857.

11 Y. Cheng, Z. Li, Y. Li, S. Dai, G. Ji, H. Zhao, J. Cao and Y. Du, *Carbon*, 2018, **127**, 643-652.

12 Z. Lou, Y. Li, H. Han, H. Ma, L. Wang, J. Cai, L. Yang, C. Yuan and J. Zou, *Acs Sustain. Chem. Eng.*, 2018, **6**, 15598-15607.